Solar Energy Materials & Solar Cells 157 (2016) 907–912

Contents lists available at ScienceDirect

Solar Energy Materials & Solar Cells

journal homepage: www.elsevier.com/locate/solmat

Anomalous photocurrent response of hybrid TiO_2:P3HT solar cells under different incident light wavelengths

Alejandro Koffman Frischknecht [c,d], Exequiel Yaccuzzi [a], Juan Plá [a], M. Dolores Perez [a,b,*]

[a] Departamento Energía Solar, GIyA, Centro Atómico Constituyentes, CNEA, CONICET Avda. Gral. Paz 1499, San Martín 1650, Buenos Aires, Argentina
[b] Escuela de Ciencia y Tecnología, Universidad Nacional de San Martín, Martín de Irigoyen No. 3100, San Martín 1650, Buenos Aires, Argentina
[c] Departamento de Electrotecnia (FAIN-UNCo), Buenos Aires 1400, 8300 Neuquén, Provincia de Neuquén, Argentina
[d] Instituto de Investigación y Desarrollo en Ingeniería de Procesos, Biotecnología y Energías Alternativas (PROBIEN, CONICET-UNCo), Neuquén, Argentina

ARTICLE INFO

Article history:
Received 15 June 2016
Received in revised form
8 August 2016
Accepted 15 August 2016

Keywords:
Hybrid solar cells
UV enhancement
Mesoporous titania

ABSTRACT

Ordered mesoporous titania present optimum optical and electronic characteristics for solar cells applications. Hybrid solar cells that combine a dye polymer and porous titania is being studied as an inexpensive alternative to solid state photoconversion devices and the role of the inorganic/organic interface is relevant to understanding the efficiency parameters. Many reports have described UV enhancement and light soaking effects for solid state hybrid cells containing titania. In this work, we study devices fabricated by incorporating P3HT into the ordered pores of a sol-gel synthesized nanocrystalline titania. We observe that the spectral response is modified upon illumination at different wavelengths. When irradiated with UV light (below 370 nm), the spectral response is drastically enhanced but when shined with visible light, the external quantum efficiency is reduced. Both effects are reversible such that several enhancement/degradation cycles can be performed. The detrimental visible light effect takes longer than the UV enhancement, which suggests a polymer mediated mechanism. Upon AM 1.5 illumination, both opposing effects are present and results in a Jsc that is sensitive to the measuring time and the test irradiation spectrum.

1. Introduction

Solid state hybrid solar cells containing titania and polymeric dyes are being studied due to the promise of cost-effective devices arising from the combination of inorganic and organic materials [1–5]. Bulk heterojunctions minimize the detrimental effects of small exciton diffusion length inherent of organic materials, and the use of titania as the electron acceptor layer additionally provides a robust matrix with tailored pores of controlled size and order [6,7]. Polymeric compounds offer the versatility of chemical synthesis to fine tune their properties and promise cost reduction. Polymers can be easily incorporated within the titania pores by simple solution methods in order to create the inorganic/organic (I/O) interface for charge separation. However, these devices have yet to demonstrate improved performances; the advantages of fabricating a device with a designed 3D inorganic structure is rapidly counterfeited by the challenges of understanding a complex I/O interface and the impact of combining donor and acceptor materials with dissimilar carrier mobilities [8–10].

Nanostructured titania has been described as an optimum material for many optoelectronic applications and photocatalysis due to its electronic, optical and structural properties [11–13]. It makes for an adequate electron acceptor and the band gap energies allow charge separation at the interface if paired with the right organic material [14–17]. Highly organized porous titania with elevated surface area can be achieved by simple sol-gel synthesis from the ethanolic Ti(IV) precursors and surfactant solution [18–21]. Upon the appropriate thermal treatment, crystalline anatase walls are obtained for sol-gel mesoporous titania that are suitable for optoelectronic applications when the substrate used is a transparent conductor electrode like ITO-covered glass [22].

Enhancement of the solar cell performance upon irradiation with UV light has been described for devices comprising titania and P3HT polymer and is a current topic of discussion [23–27]. The improvement of the photoconversion under UV light is originated at the titania layer due to the inherent electronic traps of the material. Strikingly, this effect is observed for hybrid solar cells containing titania of different nature, e.g. for thin (~10 nm)

* Corresponding author at: Departamento Energía Solar, GIyA, Centro Atómico Constituyentes, CNEA, CONICET Avda. Gral. Paz 1499, San Martín 1650, Buenos Aires, Argentina.
E-mail address: mdperez@tandar.cnea.gov.ar (M.D. Perez).

http://dx.doi.org/10.1016/j.solmat.2016.08.009
0927-0248/

amorphous TiOx [28] and for thick nanocrystalline porous titania (220 nm) typically employed in dye-sensitized solar cells [29]. This effect is a result of the population of titania defects. In parallel, copious amounts of works have dedicated extensively to the study of photoelectronic processes of rutile, anatase and amorphous titania [12,30–33]. The increase of the photocurrent upon UV light exposition for titania materials has been known for a long time, first shown for rutile in 1969 by Ghosh et al. [34]. In general, it has been fully agreed on the existence of a number of inherent defect states that correspond to shallow and deep trap levels, O vacancies and interstitial Ti^{3+}, respectively, that play a major role on the electronic conductivity [35–39].

In this report, we present the effects of monochromatic irradiation on titania/polymer heterojunction devices, both under UV and visible light, and its impact on the device spectral response. We describe opposite enhancement and degradation of the photocurrent for UV and visible light irradiation respectively. It is the first time that a distinctive visible light response has been described for this type of devices and it insinuates the possibility of use of hybrid photovoltaics as light sensing devices with specific photoresponse to the illumination wavelength.

2. Material and methods

Hybrid photovoltaic devices were fabricated with the following architecture: ITO/TiO_2 dense/TiO_2 porous: P3HT/P3HT/Ag. The titania layers (a bottom 50 nm dense layer and a top 140 nm mesoporous layer) were prepared onto an ITO-covered glass substrate using the sol-gel method from a water-ethanol solution containing a $TiCl_4$ precursor, as previously reported (sample D3M5 in Ref. [22]). Further heat treatment up to 500 °C was conducted in order to ensure high porous volume and crystalline anatase walls. The P3HT was incorporated inside the titania pores by spin coating (3000 rpm, 60 s) from the toluene solution (10 mg/mL), previous soaking for 60 s to allow penetration of the solution inside the pores. We completed 3 P3HT depositions, each one followed by thermal annealing at 200 °C for 5 min in ambient atmosphere and washing of the surface with toluene between depositions to remove the top non-infiltrated polymer and improve filling of the pore volume. A 150 nm Ag electrode was evaporated in a vacuum chamber ($P_{base}=1.10^{-5}$ Torr) through a shadow mask (device area$=7.85\times10^{-3}$ cm^2) to complete the device fabrication.

FE-SEM images were obtained with a ZEISS LEO 982 GEMINI field emission electron microscope in the secondary-electron mode, using an in-lens detector to improve resolution. Samples supported for side-view images were cut with a diamond tip in small squares and taped with an adhesive carbon tape to an L-shape aluminum support.

External quantum efficiency (EQE) and current vs. voltage (IV) measurements were performed using a calibrated InGaP reference solar cell provided by the IES (Instituto de Energía Solar – Universidad Politécnica de Madrid). InGaP was the preferred reference cell due to the similar photoresponse in the visible region of the spectrum. EQE measurements were performed with a setup composed by a Sciencetech 9055 monochromator, a Stanford Research SR380 lock-in amplifier and a Thorlabs chopper. IV measurements were carried out with a Keithley 2602 source meter and a 75 W Xenon lamp (Sciencetech) with an AM1.5 G filter as a solar simulator. The Jsc time dependence was measured using the monochromator light output at the desired wavelength.

3. Results and discussion

Devices were fabricated by incorporation of the polymer inside the titania pores by spin coating a solution of P3HT dissolved in toluene. The impregnation of the polymer within the titania matrix can be observed from the SEM images (Fig. 1A–E). For the clean titania (A and B), the top-view image reveals the open pores in a "grid-like" order structure with pore diameters of ~10 nm. The side-view image reveals how the open pores create accessible vertical channels of 10 nm diameters accordingly, with a dense (non-porous) titania layer before the ITO. The dense titania bottom layer acts as the electron transporting layer (ETL) and prevents charge recombination at the ITO interface. Images C, D and E correspond to the TiO_2:P3HT composite and reveal that the polymer is penetrating within the titania pores. From images C and D we observe that the vertical channels can no longer be distinguished and a polymer-like soft texture can be observed. The top-view image (E) reveals that a thin polymer layer remains on top of the titania that behaves as the HTL (hole transporting layer). The remaining thin 20 nm top layer is necessary as a hole conducting layer to prevent direct contact of the top metal electrode, Ag, with the porous titania. The device architecture is as follows:

ITO/TiO_2(50 nm)/TiO_2:P3HT(140 nm)/P3HT(20 nm)/Ag (150 nm) (Fig. 1F).

The typical device efficiency parameters were obtained from the measured IV curve under 1sun illumination shown in Fig. 2, Jsc$=0.47$ mA/cm^2, Voc$=0.56$ V, FF$=0.48$. The resulting efficiency ($\eta=0.12\%$) is similar to previous reports for devices employing titania: P3HT heterojunctions, even though the titania layer were reportedly obtained through different synthetic methods, with the most used material being the nanocrystalline TiO_2 deposited by doctor blade technique from its anatase paste [2,4,15,40–45]. The low efficiency is a consequence of the low Jsc; since the devices are quite thin, with only 150 nm of TiO_2:P3HT bulk film, with low illumination harvest that results in reduced absorption efficiency. Also, sol-gel synthesized titania yields pores with an amount of rather poorly interconnected pores that may prevent efficient charge extraction.

The device response to different wavelengths within the solar spectrum is characterized by its EQE presented in Fig. 2. In the visible range, the signal is originated by the photoactivity of the P3HT polymer and replicates the absorption spectral shape of a P3HT neat film. From the deconvolution analysis (presented as Supplementary material in Appendix A), the peaks of the titania and P3HT films absorption spectra can be uniquely identified and matched to the EQE maxima. The titania is responsible for the device photocurrent response in the UV region as expected from its large band gap. The lower energy bands of the titania absorption spectrum do not present photoactivity, as it is not reflected in the EQE, because they correspond to thin film interference effects. The ~440 nm titania absorption band has been assigned to mid gap states generated by oxygen vacancies [39].

The EQE signal is very sensitive to the experimental wavelength chosen to start the measurement scan. We observe that the photocurrent increases markedly when the measurement is started at wavelengths below 370 nm. Qualitatively, the effect is quick because no sustained irradiation is needed to observe an EQE enhancement, and it is long termed such that monochromatic photocurrent increase is observed throughout the entire scan. In Fig. 3 (left) we present the EQEs, by measuring the scan starting at 400 nm, typically presented in most papers, and the scan starting at 360 nm. It can be immediately observed that the EQE is drastically augmented when the initial scan wavelength is reduced and it keeps going up as further scans starting at 360 nm are performed (not shown). It must be noted that the initial EQE curves were measured on "fresh" devices, i.e. recently prepared cells with no further light exposure but the room natural illumination. UV enhancement has been reported previously, [23–27] however, those findings were observed for the IV curve under white light illumination and little is known of its effect on the spectral

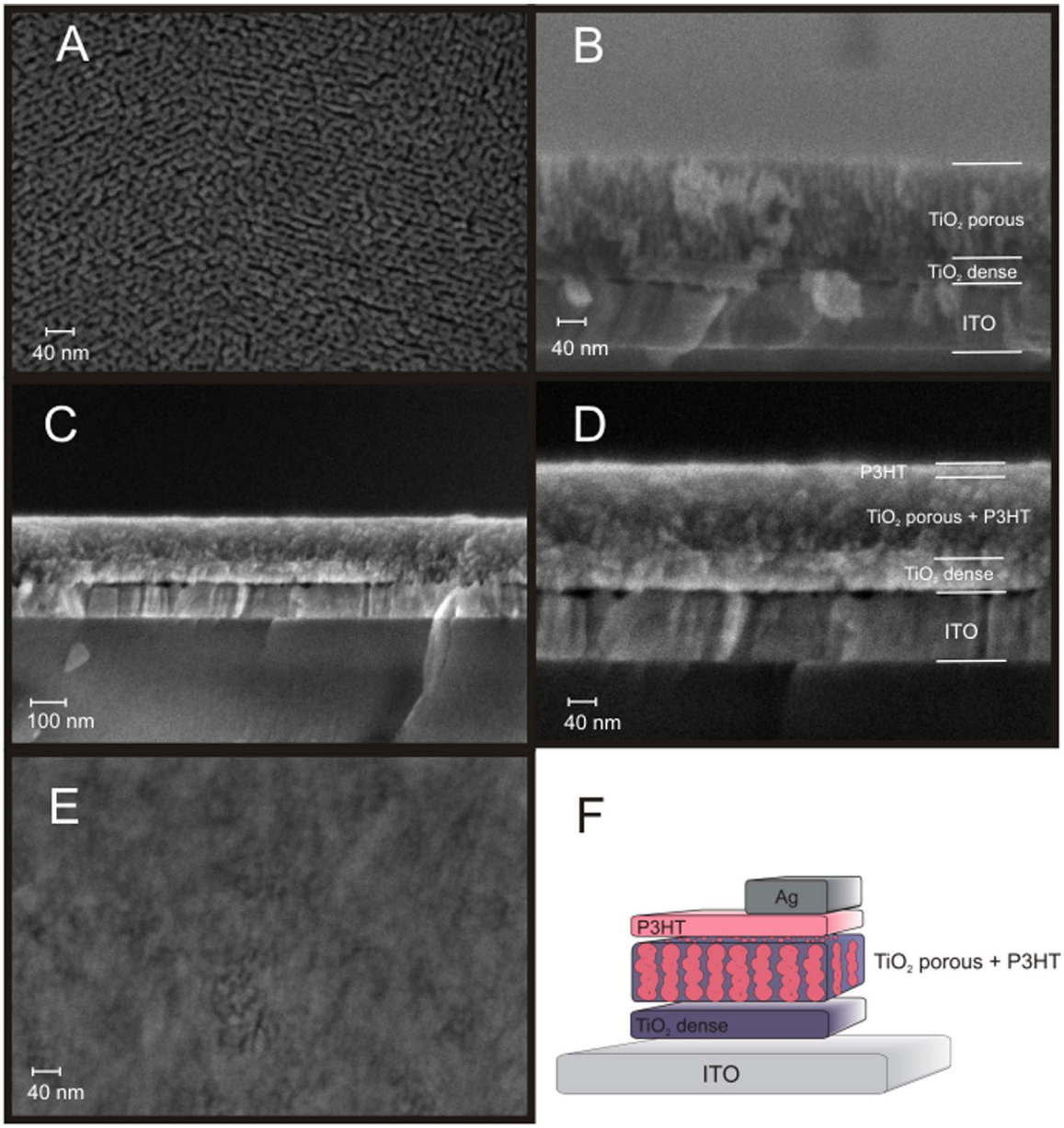

Fig. 1. (A) Top-view FE-SEM image of clean porous TiO_2. (B) Side view FE-SEM image of the titania nanostructure on ITO. (C) and (D) Side view FE-SEM images of the TiO_2:P3HT composite. (E) Top-view FE-SEM image of the TiO_2:P3HT composite. (F) Schematics of the device architecture.

response. Previous reports have assigned the UV enhancement effects observed in similar hybrid devices, to the presence of structural and electronic defects in the titania [46–49]. The sol-gel synthesized titania is a highly defective material due to the intense heat treatments necessary to remove the surfactant and to open the porosity. The 3D ordered surfactant is burned in an oxygen atmosphere into gaseous CO_2 so as to form the titania pores. When the CO_2 is expelled, it leaves oxygen vacancies in the titania walls. The absence of an oxygen atom in the titania structure produces a site with two positive charges that are localized on the Ti atoms, resulting in two possible defects, one doubly ionized oxygen vacancy (V_0^{2+}) or two singly ionized oxygen vacancies (V_0^{+}). These are shallow defects that lay very close to the conduction band (CB). The V_0^{2+} center is thermodynamically most stable and is reportedly the major defect in the bulk and surface titania. These two states are separated by $\sim$0.2 eV, such that when a photoelectron is generated with sufficient energy to populate the V_0^{2+} center, it is easily reduced to V_0^{+} [48]. The V_0^{+} center is a shallow donor that raises the Fermi level near the CB, hence, upon photoelectron trapping, the titania becomes a n-type doped semiconductor with higher electron mobilities. The result is a material with improved electronic properties that provides enhancement of the entire EQE. We studied the enhancement effect in time for a given illumination wavelength in the UV region, and observed a steep photocurrent increase as the traps become filled, followed by saturation at almost half a minute (Fig. 3, right). An astounding 400% increase in photocurrent is observed for illumination at 360 nm.

Strikingly, the opposite is observed under visible light illumination; a distinct deterioration of the EQE signal occurs when only the visible component of the spectrum reaches the device. To observe this effect, the devices were exposed to 560 nm light (the P3HT maximum absorption peak) for 10 min and yielded a reduction of the EQE signal by almost 60% (see Fig. 4). However, this effect is slower than the UV response, it is only after longer irradiation periods with visible light that the degradation becomes visible, as opposed to the UV effect. Electronic traps may also be

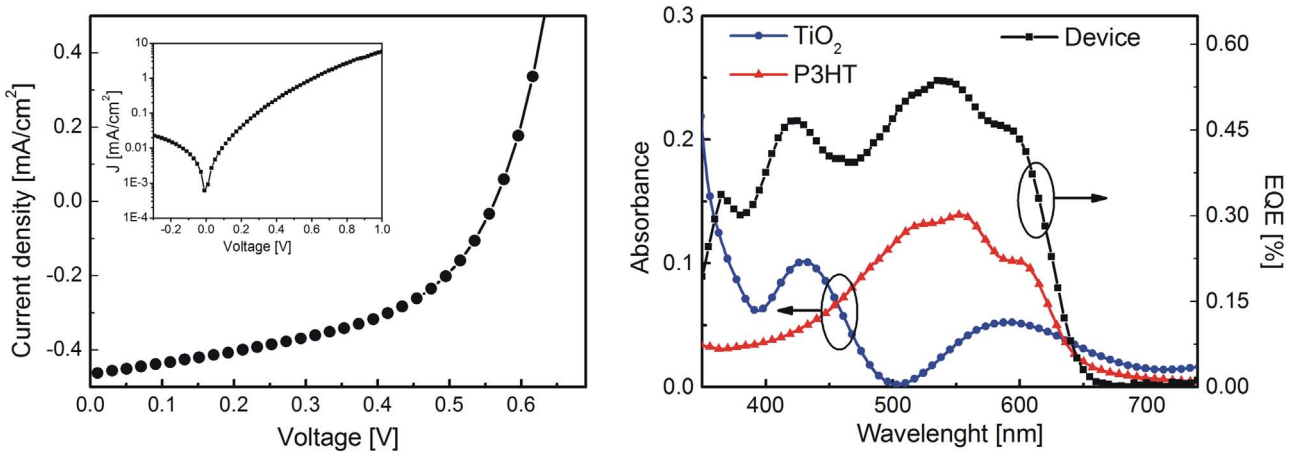

Fig. 2. Left: IV curve for dark (inset) and 1 sun illumination of the devices with structure ITO/TiO_2 (50 nm)/TiO_2:P3HT(140 nm)/P3HT(20 nm)/Ag(150 nm). Right: EQE of the device in black squares, P3HT absorption spectra in red triangles and titania absorption spectra in blue dots. (For interpretation of the references to color in this figure legend, the reader is referred to the web version of this article.)

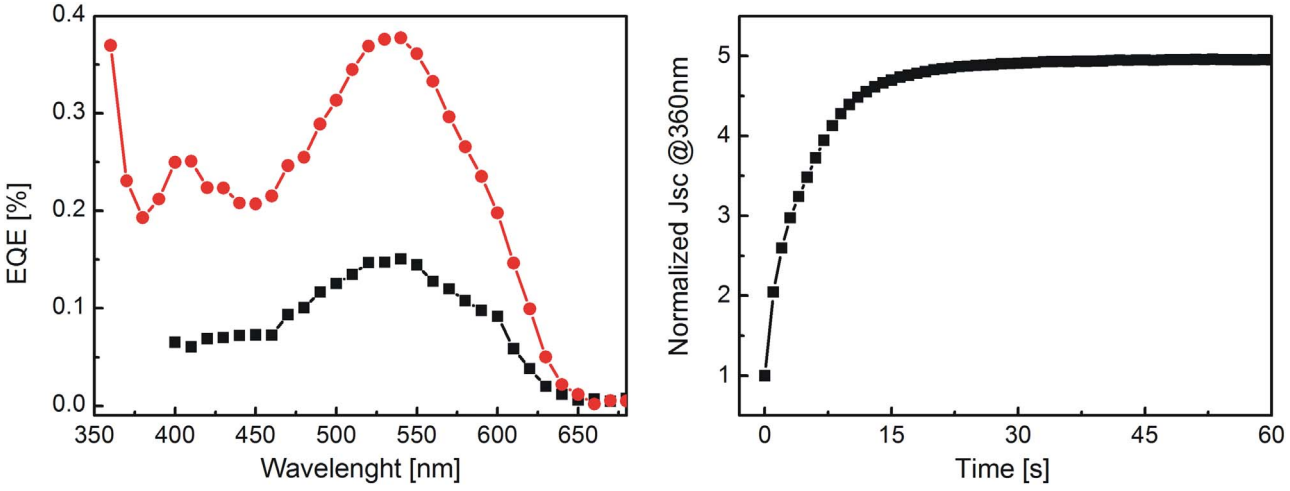

Fig. 3. Left: EQE scans initiated at different wavelengths. Right: Jsc vs. time under 360 nm monochromatic light device illumination.

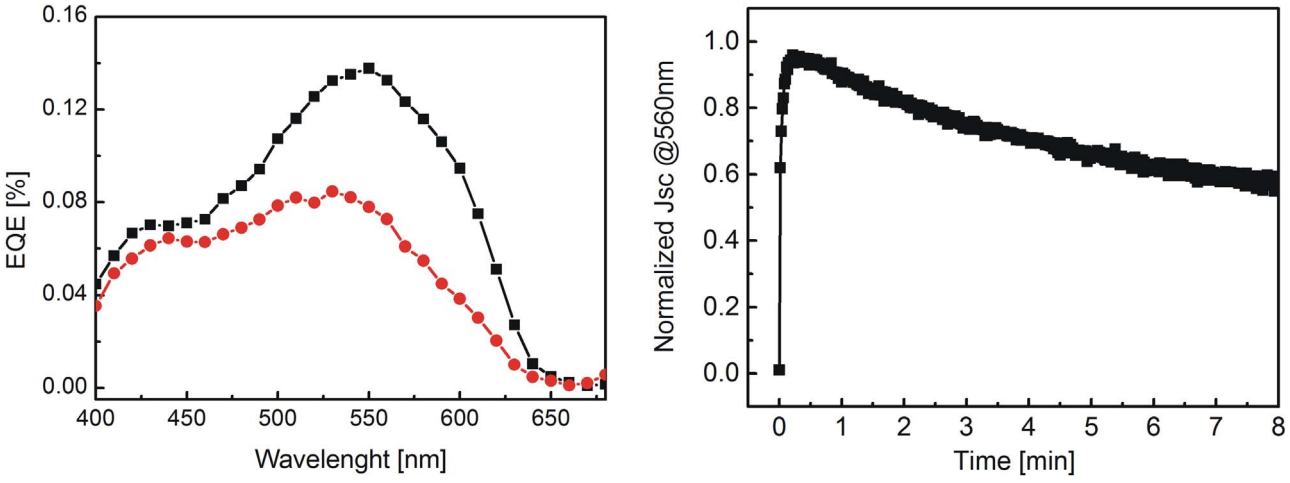

Fig. 4. Left: Original EQE (black) and after 10 min under constant 560 nm monochromatic irradiation (red). Right: Jsc vs. time under 560 nm monochromatic light device illumination. Jsc has been normalized by the Jsc (560 nm) of the original photoresponse prior to irradiation. (For interpretation of the references to color in this figure legend, the reader is referred to the web version of this article.)

responsible for this effect although they must be mediated by the P3HT excitons since the Jsc decrease is only observed for wavelengths corresponding to the polymer photoactive range. The vis-photogenerated excitons at the P3HT that reach the I/O interface will possibly recombine with the titania high mobility Vo^+ centers hence reducing the Jsc. This recombination may be slower because it competes with charge generation at the interface and it would need to involve not so efficient TiO_2:P3HT orbital overlap. This

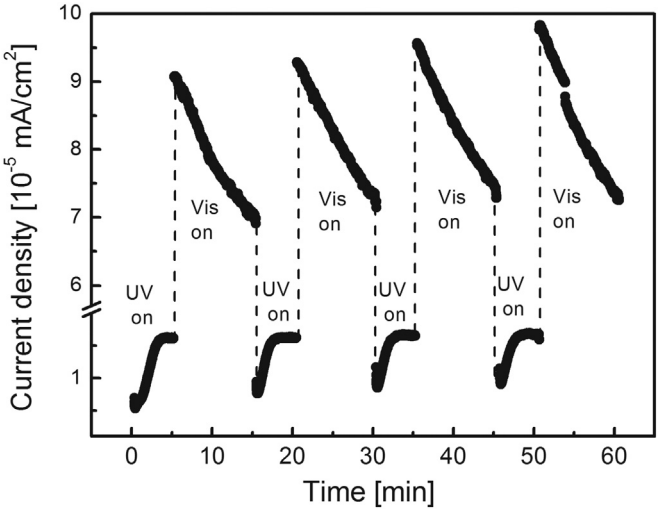

Fig. 5. Device current density under monochromatic illumination alternating wavelengths of 360 and 560 nm.

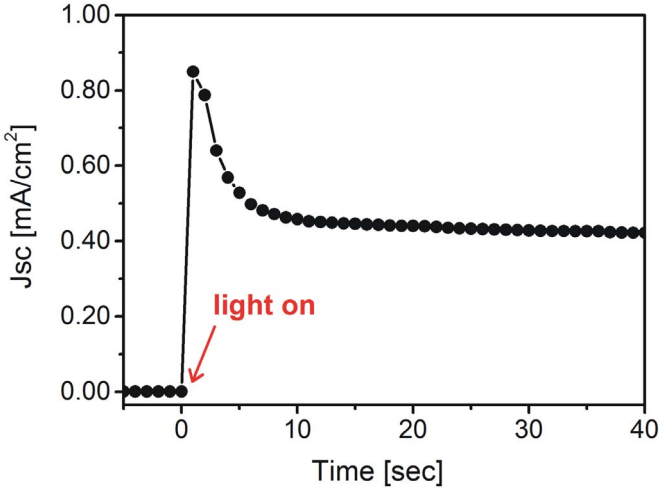

Fig. 6. Jsc vs time under AM1.5 filtered Xe lamp illumination conditions.

hypothesis should be validated experimentally in the future by a fundamental study of the material traps and charge recombination by transient spectroscopy.

The photocurrent time dependence also presents an initial slow decay due to trap depletion before it approaches a plateau as the traps become empty. We can also observe an initial short signal rise with similar characteristic time as the one at 360 nm. This could indicate that, upon light absorption of P3HT in the vicinity of the interface, there is a probability that electrons are injected into the titania surface traps, also creating an n-type doping effect. However, once recombination of titania electron traps with P3HT holes becomes important, the other effect can be disregarded and the photocurrent is reduced significantly.

Both UV enhancement and visible degradation are reversible processes and oppose each other as demonstrated in Fig. 5, where the photocurrent under successive exposition to 360 and 560 nm illuminations are presented. For 560 nm, the resulting photocurrent is about 8 times larger than the photocurrent at 360 nm due to the higher photon content of the Xe lamp spectrum and the higher responsivity of the device in the visible region. The current increases when irradiated with UV light and it decreases when illuminated with visible light. A cumulative enhancement effect is visible because consecutive cycles start at higher photocurrents. This may be originated by the fact that degradation is not sustained long enough to ensure depletion the populated traps and the material cannot return to the original trap densities.

Relaxation of the signal in the dark is also observed when illumination is turned off such that the EQE slowly goes back to the original values. This was observed for both the enhanced (UV) and the degraded (visible) curves, indicating a thermal relaxation of the populated electron traps or a repopulation of the depleted traps. The relaxation of the enhanced UV signal was reported previously and even though the relaxation times are difficult to measure because the measurement itself modifies the signal, i.e. when we illuminate the device to read the photocurrent it immediately becomes affected by it, we could observe that it takes more than 30 min for the UV enhanced signal to decay to its original value (see Supplementary material in Appendix A).

Upon white light illumination, necessary for IV curve testing and determination of the electrical parameters, both effects (UV enhancement and visible degradation) are present at the same time and cancel each other out. The resulting Jsc will depend on the time it takes to complete the IV scan and also on the amount of photons with energies within the UV and the visible region of the illumination source. When we examine the device Jsc under white light with time, we observe an initial fast photocurrent increase due to the quick UV enhancement, followed by a reduction of the photocurrent due to the visible effect that is slower and compensates the initial increase as trap recombination takes place (see Fig. 6). A Jsc stabilization is observed at times higher than 10 s, reaching a plateau where the resulting Jsc value is a result of the correlation of the number of photons of different energies and the device responsivity (absorption) to each one of them. Usually, Xe lamps with AM1.5 filters are used for efficiency measurements but sometimes other lamps can be used and the resulting effect should be acknowledged to avoid possible biased efficiencies due to high or low UV content of the lamp as compared to the solar AM1.5 spectrum. Also, it is important that each point measurement in the IV scan is taken at the time where the photocurrent has reached the plateau to avoid overestimation of the efficiency.

4. Conclusions

We have demonstrated that sol-gel synthesized mesoporous titania films used for the fabrication of hybrid solar cells present a number of electronic defects responsible for a relevant dependence of the photocurrent on the incident light wavelength and should be accounted for during signal acquisition so as not to concur in distorted results. Upon UV monochromatic illumination, the device has a strong photocurrent enhancement over the whole wavelength range due to the filling of shallow traps that become donor sites with an n-doping effect; therefore the titania electron mobilities are improved. Contrarily, when the device is illuminated with monochromatic light in the visible range, we observe a degradation of the photocurrent because of a polymer mediated recombination of the trapped titania electrons. We also determined that the typical rise/decay times are quite long such that persistent effects are observed during the entire EQE wavelength scan. This investigation has presented a new point of view for the UV-enhanced efficiency for titania-based solar cells and introduced a visible degradation effect that has been overlooked in previous reports. The reported opposite response of these devices to different regions of the solar spectrum can be used as an advantage in light sensing applications, we can envision their use as tools that present different responses in UV and visible light.

Acknowledgments

This work was funded by CNEA, and grants PIP2012–2014 No. 01052 (CONICET) and PICT2011 No. 1401 (ANPCyT). The authors are indebted to M.C. Marchi (CMA-UBA) for the SEM measurements and Galo J.A.A. Soler-Illia's Nanochemistry group for the titania films preparation facility. J. Plá and M. Dolores Perez are permanent researchers at Consejo Nacional de Investigaciones Científicas y Técnicas (CONICET). A.K. Frischknecht and E. Yaccuzzi are supported by CONICET doctoral fellowships.

Appendix A. Supplementary information

Supplementary data associated with this article can be found in the online version at http://dx.doi.org/10.1016/j.solmat.2016.08.009.

References

[1] S. Günes, N.S. Sariciftci, Hybrid solar cells, Inorg. Chim. Acta 361 (2008) 581–588.
[2] K. Naomi, H. Satoshi, S. Yuta, O. Hideo, I. Shinzaburo, B. Hiroaki, Improvement of charge injection efficiency in organic-inorganic hybrid solar cells by chemical modification of metal oxides with organic molecules, Appl. Phys. Lett. 90 (2007) 183513.
[3] Z. Rui, J. Chang-Yun, L. Bin, S. Ramakrishna, Highly efficient nanoporous TiO_2-polythiophene hybrid solar cells based on interfacial modification using a metal-free organic dye, Adv. Mater. 21 (2009) 994–1000.
[4] M. Wright, A. Uddin, Organic–inorganic hybrid solar cells: a comparative review, Sol. Energy Mater. Sol. Cells 107 (2012) 87–111.
[5] T. Xu, Q. Qiao, Conjugated polymer–inorganic semiconductor hybrid solar cells, Energy Environ. Sci. 4 (2011) 2700–2720.
[6] P. Heremans, D. Cheyns, B.P. Rand, Strategies for increasing the efficiency of heterojunction organic solar cells: material selection and device architecture, Acc. Chem. Res. 42 (2009) 1740–1747.
[7] J. Roncali, Molecular bulk heterojunctions: an emerging approach to organic solar cells, Acc. Chem. Res. 42 (2009) 1719–1730.
[8] I. Haeldermans, K. Vandewal, W.D. Oosterbaan, A. Gadisa, J. DaHaen, M.K. Van Bael, J.V. Manca, J. Mullens, Ground-state charge-transfer complex formation in hybrid poly(3-hexyl thiophene): titanium dioxide solar cells, Appl. Phys. Lett. 93 (2008) 223302.
[9] A. Panda, C.K. Renshaw, A. Oskooi, K. Lee, S.R. Forrest, Excited state and charge dynamics of hybrid organic/inorganic heterojunctions. II. Experiment, Phys. Rev. B 90 (2014) 045303.
[10] C.K. Renshaw, S.R. Forrest, Excited state and charge dynamics of hybrid organic/inorganic heterojunctions. I. Theory, Phys. Rev. B 90 (2014) 045302.
[11] Y. Bai, I. Mora-Seró, F. De Angelis, J. Bisquert, P. Wang, Titanium dioxide nanomaterials for photovoltaic applications, Chem. Rev. 114 (2014) 10095–10130.
[12] A. Fujishima, X. Zhang, D.A. Tryk, TiO_2 photocatalysis and related surface phenomena, Surf. Sci. Rep. 63 (2008) 515–582.
[13] J. Schneider, M. Matsuoka, M. Takeuchi, J. Zhang, Y. Horiuchi, M. Anpo, D. W. Bahnemann, Understanding TiO_2 photocatalysis: mechanisms and materials, Chem. Rev. 114 (2014) 9919–9986.
[14] S. Agarwala, M. Kevin, A.S.W. Wong, C.K.N. Peh, V. Thavasi, G.W. Ho, Mesophase ordering of TiO_2 film with high surface area and strong light harvesting for dye-sensitized solar cell, ACS Appl. Mater. Interfaces 2 (2010) 1844–1850.
[15] K.M. Coakley, M.D. McGehee, Photovoltaic cells made from conjugated polymers infiltrated into mesoporous titania, Appl. Phys. Lett. 83 (2003) 3380–3382.
[16] M. Rawolle, K. Sarkar, M.A. Niedermeier, M. Schindler, P. Lellig, J.S. Gutmann, J.-Fo Moulin, M. Haese-Seiller, A.S. Wochnik, C. Scheu, P. Muller-Buschbaum, Infiltration of polymer hole-conductor into mesoporous titania structures for solid-state dye-sensitized solar cells, ACS Appl. Mater. Interfaces 5 (2013) 719–729.
[17] H. Wang, C.C. Oey, A.B. Djurisic, M.H. Xie, Y.H. Leung, K.K.Y. Man, W.K. Chan, A. Pandey, J.-M. Nunzi, P.C. Chui, Titania bicontinuous network structures for solar cell applications, Appl. Phys. Lett. 87 (2005) 023507.
[18] P.C. Angelomé, L. Andrini, M.E. Calvo, F.G. Requejo, S.A. Bilmes, G.J.A.A. Soler-Illia, Mesoporous anatase TiO_2 films: use of Ti K XANES for the quantification of the nanocrystalline character and substrate effects in the photocatalysis behavior, J. Phys. Chem. C. 111 (2007) 10886–10893.
[19] X. Chen, S.S. Mao, Titanium dioxide nanomaterials: synthesis, properties, modifications, and applications, Chem. Rev. 107 (2007) 2891–2959.
[20] A.G. Macedo, L.L. Mattos, E.R. Spada, R.B. Serpa, C.S. Campos, I.R. Grova, L. Ackcelrud, Fo.T. Reis, M.L. Sartorelli, L.S. Roman, Preparation of porous titanium oxide films onto indium tin oxide for application in organic photovoltaic devices, Appl. Surf. Sci. 258 (2012) 5375–5379.
[21] G.J.A.A. Soler-Illia, O. Azzaroni, Multifunctional hybrids by combining ordered mesoporous materials and macromolecular building blocks, Chem. Soc. Rev. 40 (2011) 1107–1150.
[22] I.L. Violi, M.D. Perez, M.C. Fuertes, G.J.A.A. Soler-Illia, Highly ordered, accessible and nanocrystalline mesoporous TiO_2 thin films on transparent conductive substrates, ACS Appl. Mater. Interfaces 4 (2012) 4320–4330.
[23] L. Cabau, L. Pelleja, J.N. Clifford, C.V. Kumar, E. Palomares, Light soaking effects on charge recombination and device performance in dye sensitized solar cells based on indoline-cyclopentadithiophene chromophores, J. Mater. Chem. A 1 (2013) 8994–9000.
[24] A. Guerrero, S. Chambon, L. Hirsch, G. Garcia-Belmonte, Light-modulated TiOx interlayer dipole and contact activation in organic solar cell cathodes, Adv. Funct. Mater. 24 (2014) 6234–6240.
[25] T. Kuwabara, T. Nakayama, K. Uozumi, T. Yamaguchi, K. Takahashi, Highly durable inverted-type organic solar cell using amorphous titanium oxide as electron collection electrode inserted between ITO and organic layer, Sol. Energy Mater. Sol. Cells 92 (2008) 1476–1482.
[26] M.R. Lilliedal, A.J. Medford, M.V. Madsen, K. Norrman, F.C. Krebs, The effect of post-processing treatments on inflection points in current–voltage curves of roll-to-roll processed polymer photovoltaics, Sol. Energy Mater. Sol. Cells 94 (2010) 2018–2031.
[27] H. Schmidt, K. Zilberberg, S. Schmale, H. Flugge, T. Riedl, W. Kowalsky, Transient characteristics of inverted polymer solar cells using titanium oxide interlayers, Appl. Phys. Lett. 96 (2010) 243305.
[28] J. Kim, G. Kim, Y. Choi, J. Lee, S. Heum Park, K. Lee, Light-soaking issue in polymer solar cells: Photoinduced energy level alignment at the sol-gel processed metal oxide and indium tin oxide interface, J. Appl. Phys. 111 (2012) 114511.
[29] P. Ravirajan, P. Atienzar, J. Nelson, Post-processing treatments in hybrid polymer/titanium dioxide multilayer solar cells, J. Nanoelectron. Optoelectron. 7 (2012) 498–502.
[30] M.C. Fravventura, L.D.A. Siebbeles, T.J. Savenije, Mechanisms of photogeneration and relaxation of excitons and mobile carriers in anatase TiO_2, J. Phys. Chem. B 118 (2014) 7337–7343.
[31] M.H. Rittmann-Frank, C.J. Milne, J. Rittmann, M. Reinhard, T.J. Penfold, M. Chergui, Mapping of the photoinduced electron traps in TiO_2 by picosecond x-ray absorption spectroscopy, Angew. Chem. Int. Ed. 53 (2014) 5858–5862.
[32] S.H. Szczepankiewicz, A.J. Colussi, M.R. Hoffmann, Infrared spectra of photoinduced species on hydroxylated titania surfaces, J. Phys. Chem. B 104 (2000) 9842–9850.
[33] S.H. Szczepankiewicz, J.A. Moss, M.R. Hoffmann, Slow surface charge trapping kinetics on irradiated TiO_2, J. Phys. Chem. B 106 (2002) 2922–2927.
[34] A.K. Ghosh, F.G. Wakim, R.R. Addiss, Photoelectronic processes in rutile, Phys. Rev. 184 (1969) 979–988.
[35] C. Di Valentin, G. Pacchioni, A. Selloni, Electronic structure of defect states in hydroxylated and reduced rutile TiO_2 (110) surfaces, Phys. Rev. Lett. 97 (2006) 166803.
[36] C. Di Valentin, G. Pacchioni, A. Selloni, Reduced and n-type doped TiO_2: nature of Ti3+ species, J. Phys. Chem. C. 113 (2009) 20543–20552.
[37] E. Finazzi, C. Di Valentin, G. Pacchioni, Nature of Ti interstitials in reduced bulk anatase and rutile TiO_2, J. Phys. Chem. C. 113 (2009) 3382–3385.
[38] C.C. Mercado, F.J. Knorr, J.L. McHale, S.M. Usmani, A.S. Ichimura, L.V. Saraf, Location of hole and electron traps on nanocrystalline anatase TiO_2, J. Phys. Chem. C. 116 (2012) 10796–10804.
[39] Y. Tamaki, K. Hara, R. Katoh, M. Tachiya, A. Furube, Femtosecond visible-to-IR spectroscopy of TiO_2 nanocrystalline films: elucidation of the electron mobility before deep trapping, J. Phys. Chem. C 113 (2009) 11741–11746.
[40] A. Abrusci, I.K. Ding, M. Al-Hashimi, T. Segal-Peretz, M.D. McGehee, M. Heeney, G.L. Frey, H.J. Snaith, Facile infiltration of semiconducting polymer into mesoporous electrodes for hybrid solar cells, Energy Environ. Sci. 4 (2011) 3051–3058.
[41] C.H. Wu, H. Li, H.H. Fong, V.A. Pozdin, L.A. Estroff, G.G. Malliaras, Room-temperature preparation of crystalline TiO_2 thin films and their applications in polymer/TiO_2 hybrid optoelectronic devices, Org. Electron. 12 (2011) 1073–1079.
[42] N.J. Gerein, M.D. Fleischauer, M.J. Brett, Effect of TiO_2 film porosity and thermal processing on TiO 2P3HT hybrid materials and photovoltaic device performance, Sol. Energy Mater. Sol. Cells 94 (2010) 2343–2350.
[43] H.J. Her, J.M. Kim, C.J. Kang, Y.S. Kim, Hybrid photovoltaic cell with well-ordered nanoporous titania-P3HT by nanoimprinting lithography, J. Phys. Chem. Solids 69 (2008) 1301–1304.
[44] W.P. Liao, S.C. Hsu, W.H. Lin, J.J. Wu, Hierarchical TiO_2 nanostructured array/P3HT hybrid solar cells with interfacial modification, J. Phys. Chem. C 116 (2012) 15938–15945.
[45] M. Planells, A. Abate, H.J. Snaith, N. Robertson, Oligothiophene interlayer effect on photocurrent generation for hybrid TiO_2/P3HT solar cells, ACS Appl. Mater. Interfaces 6 (2014) 17226–17235.
[46] B.J. Morgan, G.W. Watson, Intrinsic n-type defect formation in TiO_2: a comparison of rutile and anatase from GGA+U calculations, J. Phys. Chem. C 114 (2010) 2321–2328.
[47] J. Nowotny, Titanium dioxide-based semiconductors for solar-driven environmentally friendly applications: impact of point defects on performance, Energy Environ. Sci. 1 (2008) 565–572.
[48] T. Yamamoto, T. Ohno, A hybrid density functional study on the electron and hole trap states in anatase titanium dioxide, Phys. Chem. Chem. Phys. 14 (2012) 589–598.
[49] H.X. Zhu, P.X. Zhou, X. Li, J.M. Liu, Electronic structures and optical properties of rutile TiO_2 with different point defects from DFT+U calculations, Phys. Lett. 378 (2014) 2719–2724.